RES MILITARIS
REVUE EUROPEENNE D ETUDES EUROPEAN JOURNAL OF MILITARY STUDIES
Social Science Journal

Evaluation Of Inelastic Behavior and Performance Level of Existing Structure 31 Stories in Surabaya Using Non-Linear Time History Analysis

By

Nur Achmad Husin
Department of Civil Infrastructure Engineering, Sepuluh Nopember Institute of Technology, Surabaya, Indonesia
Email: nahusin@ce.its.ac.id

Arif Paramananda Faros
Department of Civil Infrastructure Engineering, Sepuluh Nopember Institute of Technology, Surabaya, Indonesia

Ibnu Pudji Rahardjo
Department of Civil Infrastructure Engineering, Sepuluh Nopember Institute of Technology, Surabaya, Indonesia

Dicky Imam Wahyudi, Sungkono
Department of Civil Infrastructure Engineering, Sepuluh Nopember Institute of Technology, Surabaya, Indonesia

Yuyun Tajunnisa
Department of Civil Infrastructure Engineering, Sepuluh Nopember Institute of Technology, Surabaya, Indonesia
Email: yuyun_t@ce.its.ac.id

Abstract

This study evaluates the inelastic behavior and performance level of existing 31-stories buildings in Surabaya using the non-linear time history analysis (NLTHA). The evaluation was conducted because of some SNI 1726-2019 regulation changes. The selection of time history data adjusts to the characteristics of the Surabaya earthquake area through the response spectrum, magnitude, and slip mechanism. The predicted inelastic response from response spectrum analysis (RSA) will be compared to the actual inelastic response of non-linear time history analysis (NLTHA). The results of NLTHA show that the structure's performance level belongs to the life safety category (LS) category with a maximum drift ratio of 1.1%. Beam hinges exceed the maximum limit of immediate occupancy (IO) level. The maximum yielding moment ratio is 1.05. The maximum plastic rotation that occurs is 0.73%. Response reduction, inelastic deformation enlargement, and overstrength factors R, Cd, and Ω are 6.11, 4.74, and 1.82, respectively.

Keywords — building, seismic, time-history, hinges, inelastic, performance level

Introduction

The design standards for earthquake-resistant buildings are always changing in updating data and provisions over time based on the results of the evaluation by the National Standards Agency. Presently, the most recent change in seismic design standards for the building is SNI 1726-2019. The PGA value stated in SNI 1726-2012 is lower than the PGA

value involving the Kendeng Fault earthquake source from the results of deterministic seismic analysis [1].

The building exists in Surabaya which is designed by using SNI 1726-2012 standard. An evaluation is needed to investigate the condition of the structure based updated standard which is SNI 1726-2019. Building structures with vertical irregularities or structures with a height exceeding 48m and having height mode effect, the analytical procedure that can be used to evaluate the performance is a non-linear dynamic analysis of time history [2], [3].

At least 5-time history earthquake data are required, which are modified in such a way that the magnitude is close to the response spectrum of the target [4], [5]. Earthquakes are modeled by recording actual earthquakes in the form of *ground motion* which is selected based on the approach to the characteristics of the fault mechanism source, magnitude, epicenter, and the shape of the response spectrum [6]. In this case, the earthquake that may cause maximum shock to the structure is the Kendeng fault in Surabaya area, with a maximum potential magnitude of 6.5 Mw[7]–[10].

Literature Review

2.1 Linear and Nonlinear Analysis

Standard used in seismic design of building structures is designed that structure does not exceed the elastic deformation limit. So, the building can return to its balanced position. If structure deforms and exceeds the elastic condition, it cannot return to its original condition. In these conditions, a non-linear analysis procedure is needed to determine the inelastic behavior of a structure. The non-linear analysis considers plastic deformation, which affects the degradation stiffness properties of the structure [7].

2.2 Plastic Hinges

The structure that receives earthquake loads at a level exceeds elastic limits will occur plastic hinges at the ends of beams and bottom base of the column. A plastic hinge is a plastic form of beam or column inability to resist more forces under plastic deformation conditions[11].

A structure's design must follow the design concept of strong columns and weak beams. This can be achieved when there is a plastic hinge at the beam's ends and the column's bottom base. This design concept is intended the structure that receives earthquake loads at a level exceeding elastic limit will have plastic hinges at the ends of the beams and the bottom base of the column. A plastic hinge is a plastic form of beam or column inability to resist more forces under plastic deformation conditions to mean that if a structure collapses, the beam will collapse first. If the column collapses first, building will collapses immediately [7]. So, the structure is well designed when plastic hinge occurred in beams early than columns.

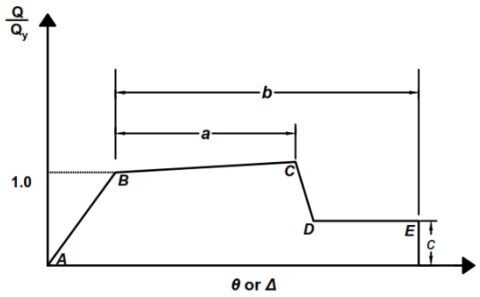

Figure 1. *Plastic hinge yielding according to FEMA 356*

Figure 1 explain that plastic hinges due to bending moments occur in beam if the working load exceeds the yield bending moment capacity (point B)[11]. Therefore, the plastic hinge will yield up to its maximum capacity (110%), accompanied by plastic rotation until the point of collapse (point C) according to FEMA-356.

2.3 Ductility

Structure ductility is the ability of a structure to deform on a large scale without experiencing sudden collapse or brittle failure. With the availability of this capability, the building will maintain its collapse in post-elastic deformation due to alternating earthquake loads. The ductility of a structure is symbolized by μ. The value of structure's ductility can be obtained from ratio between roof displacement ultimate condition and yield condition [12], [13]. The description is formulated in equation 1.

$$\mu = \frac{\delta u}{\delta y} \qquad (1)$$

Description

- μ = ductility
- δu = top floor drift at ultimate condition
- δy = top floor displacement at yielding condition

2.4 Response Modification Factor

Modification factor R is a factor that reduces the design earthquake so that the expected structural design can behave in a ductile behaviour. The value of R depends on three factors which is *over-strength, ductility, and redundancy* [13], [14]. Behavior factor (R) is determined by SNI 1726-2019 seismic standard as 7 for dual system with concrete shear wall.

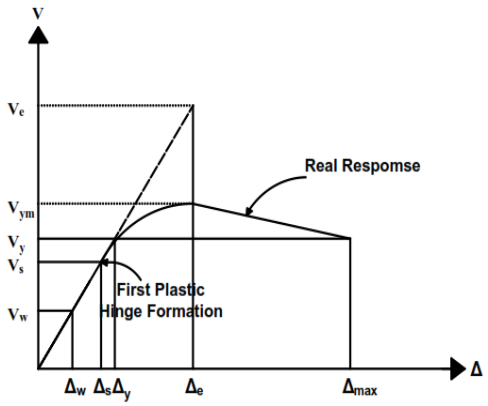

Figure 2. *Building Structure Response*

The inelastic behavior of structure is explained on Figure 2 which is idealized as an elastic-plastic bilinear relationship. Base shear force yielding condition is expressed in *Vy* and rood displacement yielding condition is expressed in Δy. *Ve* represents shear force from dynamic linear analysis (without reduction) or response spectrum analysis (RSA)[13].

The ratio of *Ve* to *Vy* is response reduction factor by the structure ductility expressed in Rμ and modeled in equation 2.

$$R_\mu = \frac{V_e}{V_y} \qquad (2)$$

Besides, there are *over-strength* and *redundancy factors* (enlargement) which affect response reduction factor [13]. The over-strength factor is expressed by ratio of *Vy* to *Vs* which modeled in equation 3.

$$R_s = \frac{V_y}{V_s} \qquad (3)$$

So, the formula of response reduction factor which depends on ductility and over-strength factor is modelled in equation 4.

$$R = R_\mu \, x \, R_s \qquad (4)$$

Description:

- *Ve* = maximum base shear force elastic ultimate
- *Vy* = base shear force structure yields condition
- *Vs.* = base shear force when element experiences its first yield
- R_μ = response reduction factor due to ductility
- R_s = response reduction factor due to over-strength
- R = response reduction of structure

2.5 Structure Performance Level

Structure of building has a level of structure performance against earthquake resistance. The criteria for accepting performance levels follows the standard requirements which determined by *the Federal Emergency Management Agency* (FEMA) and the *Applied Technology Council* (ATC).

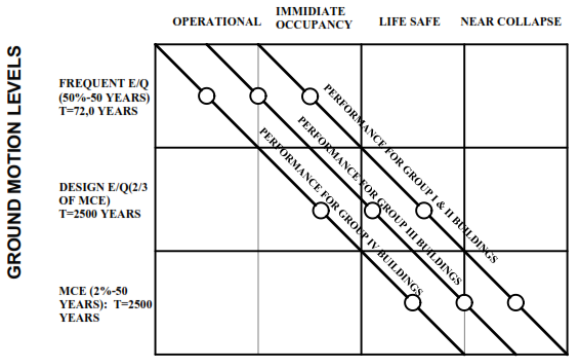

Figure 3. *Acceptance criteria of performance level based on FEMA-356*

The performance level of the structure is shown in Figure 3 with the definitions described in the points below[15], [16].

- *Immediate Occupancy* (IO): If an earthquake occurs the structure is still safe and there is only a small amount of minor damage, which to repair does not disturb the user.
- *Life Safety* (LS): When an earthquake occurs, the structure is significantly damaged but has not yet collapsed, the main structural components do not collapse, and the structure is stable enough to withstand another earthquake. The building can still be used if repairs are made.
- *Collapse Prevention* (CP): A condition that limits the structure's ability where the structural and non-structural have suffered severe damage, but the structure remains to stand and does not collapse. The structure is no longer able to withstand lateral forces.

Meanwhile, based on ATC-40, the performance level of the structure is shown in Figure 4.

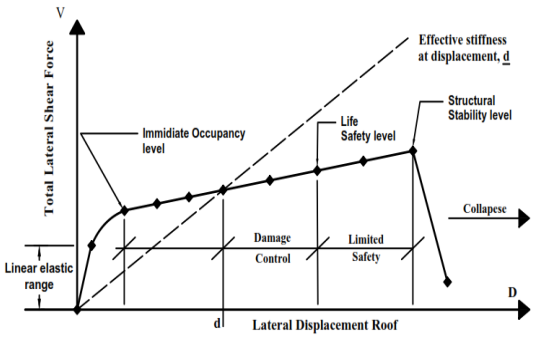

Figure 4. *Performance level based on ATC-40*

The performance level qualifications which determined by ATC-40 have similar performance level description to FEMA-356, but there are several different terms, such as *damage control, limited safety, and structural stability*. The three levels are described in the points below.

- *Damage Control*: The structural damage that occurs between IO and LS. This level can better limit the structural damage that occurs to buildings than LS.
- *Limited safety*, the existing building level is not as good as Life Safety and not as bad as *Structural Stability*.
- *Structural Stability*, Has the same description as *Collapse Prevention.*

According to requirements of FEMA-356 and ATC-40, performance level of strucutre can be classified through an aspect of its inelastic drift ratio. The *drift ratio limit* for each performance level is shown in table 1.

Table 1. *Drift ratio limit of each performance level*

Element	Aspect	CP	LS	IO
Frame system (beam-column)	Drift %	4%	2%	1%

Methodology

3.1 Working Flow

The stages of work carried out in this study began with collecting and determining the response spectrum of the Surabaya area target by following the provisions of SNI 1726-2019. In addition, the characteristics of the earthquake source in the Surabaya area were identified through the Kendeng Fault, which is the closest earthquake source to the location of the building site. Five-time history earthquakes were selected, taking into account the characteristics of the magnitude, *slip mechanism*, epicenter distance, and shape of the response spectrum. The time history chosen earthquake is scaled in magnitude to the response of the target spectrum by *amplitude method scaling* and *spectral matching*.

Linear analysis was carried out to evaluate the response and capacity of structural elements to the design earthquake update. Predicted inelastic response and load capacity exceeding element capacity were verified against time history non-linear analysis.

Time history analysis was carried out to obtain the actual inelastic conditions. So, the inelastic *drift* response can be known. The load capacity that exceeds the yield capacity of the element is observed for the degree of plastification and its failure through plastic hinges. The overall response of the structure is depicted by employing a graph of the relationship between the *base-shear* and the *roof displacement*. The response modification factors expressed in R, Cd, and Ω can be obtained by knowing the elastic limits and plastic peaks.

3.2 Building Information Data

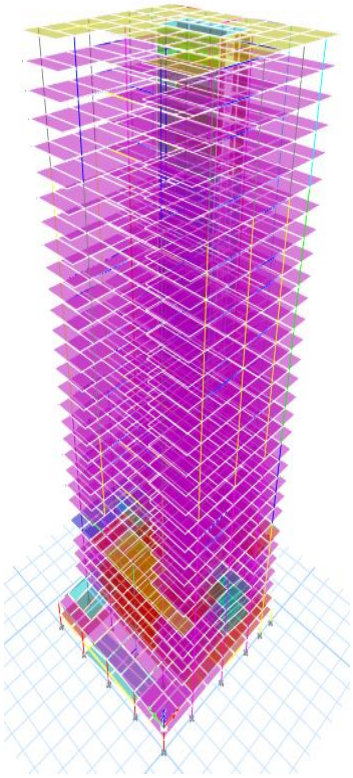

Figure 5. *3D View of Structure Model*

The research object used is a 31-story apartment building in Surabaya with technical data described in the details below.

- Number of Floors : 31 Floors
  - Podium : 1-6 Floor
  - *Low level* : 7-11 Floor
  - *Medium level* : 12-26 Floor
  - *High level* : 27-31 Floor
- Building Height : 85.90 m (from the road)
- Structure System : Dual System - *Core Wall*
- Soil Site Class : Soft Soil (SE)

3.3 Selected Time History

Geographically, Surabaya is located on two faults that may active which are Kendeng fault and Waru fault, with a magnitude of 6.5. The Kendeng Fault crosses the centre of Surabaya and moves 0.05 mm/year. Thus, PUSGEN 2017 describes characteristics of the earthquake source in the Surabaya area are detailed in table 2.

Table 2. *Characteristics of Surabaya earthquake area based on PUSGEN*

Fault	Movement (mm/year)	Mechanism	Maximum magnitude
Kendeng	0.05	*Reverse-slip*	6.5

Ground motion recorded data in form of accelerograms were selected based on criteria that were adjusted to the characteristics of Surabaya seismic zone. Ground motion data in form of accelerograms were obtained through PEER website based on magnitude, mechanism of earthquake source, distance to the site, and characteristic of spectrum response[4], [5], [17], [18]. Selected ground motions were obtained as follow in table 3.

Table 3. *Selected time history data*

Earthquake history	Year	Station	Fault mechanism	R_{JB} km	Magnitude (Mw)
Northridge-01	1994	Canoga Park - Topanga Can	*Reverse-slip*	13.1	6.6
Christchurch, New Zealand	2011	Christchurch Resthaven	*Reverse-slip*	17.86	6.2
Chuetsu-oki, Japan	2007	Kashiwazaki NPP	*Reverse-slip*	9.4	6.8
Taiwan	1983	SMART1- I01	*Reverse-slip*	95.7	6.5
Friuly, Italy-01	1976	Codroipo	*Reverse-slip*	33.32	6.5

3.4 Modification of Amplitude Scaling

The process of modifying or scaling time history data is carried out to equalize the magnitude of ground acceleration imposed in evaluation stage of existing structure, it brings evaluation closer to the design. The ground motion must be scaled in amplitude *scaling* or spectrally matched (*spectral matching*) according to the requirements convergently [17]. Each ground motion must be scaled, with the same scale factor applied to both horizontal components, so the average of the maximum directional spectra of all ground motions generally matches or exceeds the target response spectra over the specified time range[4], [5], .

Table 4. *Determination of the specified period range[13]*

	0.149 - 4.572 seconds		
Determinant Period Range	$T1_{\_}$	3.048	s
	T_3	1,837	s
	T_{18}	0.149	s
	$T_{.bottom}$	0.149	s
	$T_{.bottom.max}$	**0.2T (3)**	s
	OK	0.3674	S
	$T_{.top}$	4,572	s
	$T_{.top.min}$	**1.5 T (1)**	

Description of table 4 are,

- **T1** = The largest first period of the structure from both horizontal directions that occurs in the first mode.
- **T3** = The largest first period of the structure from both horizontal directions that occurs in the third mode.
- **T_{18}** = The smallest first period of the structure when it reaches 90% mass participation from both horizontal directions, which occurs in the 18th mode.

- **Sa (actual)** = Earth acceleration time history spectrum response acceleration.
- **Sa (target)** = Acceleration of the earthquake spectrum response SNI 1726-2019 or SNI 1726-2012

$$\alpha = \frac{\sum_{T=T_B}^{T_A}\left(S_a^{aktual} \, x \, S_a^{target}\right)}{\sum_{T=T_B}^{T_A}\left(S_a^{aktual}\right)^2} \qquad (5)$$

Note:

- Sa (actual) = time history spectral acceleration
- Sa (actual) = acceleration spectral response of the target spectrum

This scaling method gives the same magnitude for the entire earthquake period[19]. The advantage of adjustment with this method is that the characteristic nature of the selected ground motion record does not change. The scale of each ground motion is adjusted to the target's response spectra described in table 5 with the scale obtained from equation 5.

Table 5. *Scale of time history load with amplitude scaling method*

No.	Earthquake History Name	Target Spectrum Response		Determining Period Tb	-	ta	Scale
1	Northridge-01	DBE	SNI 1726-2019	0.15	-	4,572	**1,199**
2	Christchurch, New Zealand	DBE	SNI 1726-2019	0.15	-	4,572	**0.751**
3	Chuetsu-oki, Japan	DBE	SNI 1726-2019	0.15	-	4,572	**0.844**
4	Taiwan	DBE	SNI 1726-2020	0.15	-	4,572	**11.14**
5	Friuly, Italy-01	DBE	SNI 1726-2021	0.15	-	4,572	**4,417**

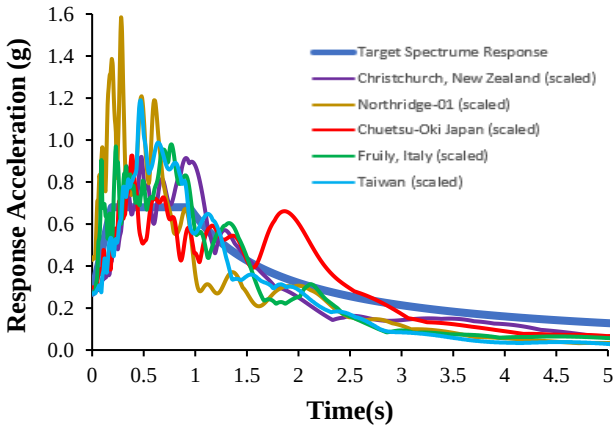

Figure 6. *The result of modification with amplitude scaling method*

3.5 Modification of Spectral Matching

Spectral matching method is an attempt to get closer or adjust the real recorded ground motion to the target spectrum response designed with SNI 1726-2019 by scaling it in such a way that the ground motion spectrum response approaches the shape of the target spectrum response in the specified period range (0.2T-1.5T) [18], [20].

In this method, the modifying and scaling were not done manually but using the ETABS program. Input data that needed are ground acceleration time history and target spectrum response (2019). Spectral matching scaling is carried out in period adjustment to obtain

maximum adjustment results even though it loses the natural properties of the actual earthquake record.

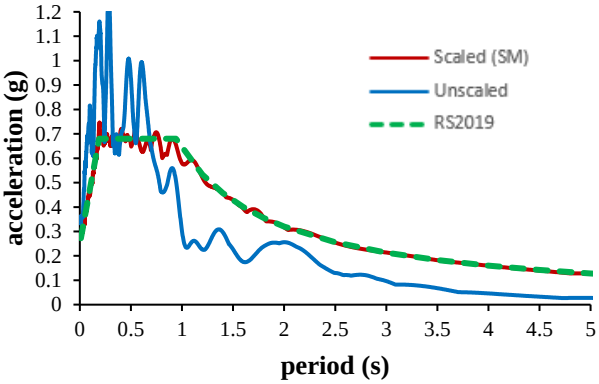

Figure 7. *The result of of modification with spectral matching*

Results And Discussion

4.1 Respon Spectrum Analysis Results

The story drift(Δ) shall be calculated as difference in drift of the center of mass above and below floor level under consideration[21], [22]. Suppose the center of mass is not aligned in the vertical direction. In that case, it is permitted to calculate the drift at the bottom of the story based on the vertical projection of the center of mass of the story above.

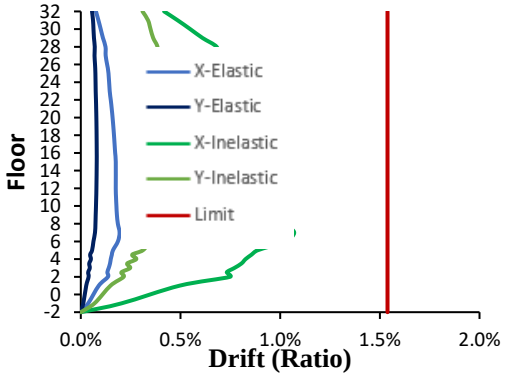

Figure 8. *Interstory drift ratio because of SNI 1726-2019*

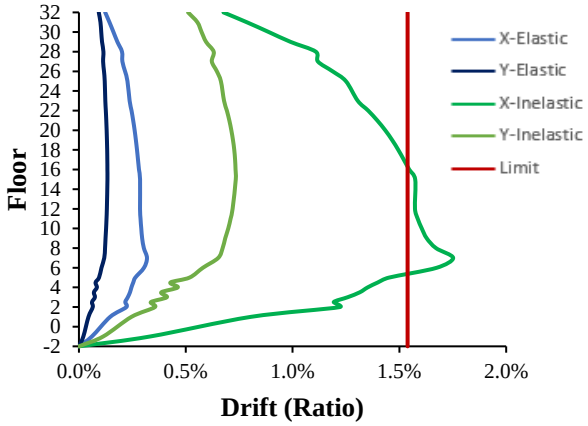

Figure 9. *Interstory drift ratio because of SNI 1726-2012*

Figures 8 and 9 show that the structure does not meet the limit of the permitted interstory drift due to changes in the design earthquake force in SNI 1726-2019. This is because the predicted inelastic drift exceeds the maximum allowable Limit (2%) [15], [21]. This event will be verified using a non-linear analysis of the time history by considering the story drift of the actual inelastic condition.

Meanwhile, in the aspect of the ability of structural elements, several controls were carried out on the main structural elements, namely beams and columns. Control results are tabulated in table 6.

Table 6. *Capacity control of elements according to seismic standards*

Structure Element	Description	Sni 1726-2012	Sni 1726-2019
BEAM	Bending moment control	Fulfill	It does not meet the requirement
	Special shear strength design	Fulfill	Fulfill
COLUMN	Axial-bending control	Fulfill	Fulfill
	Special shear strength design	Fulfill	Fulfill
CORE-WALL	Bending capacity	-	Fulfill
	Shear capacity	-	Fulfill

4.2 Non-linear Time History Analysis Results

The maximum interstory drift each floor generates in the five earthquakes. Both scaling method show that the shape of relationship is the same. Interstory drift response in x-axis is greater than the y-axis. In addition, the story drift response generated from the spectral method matching is bigger than the amplitude method scaling.

A. Inelastic drift between levels

Figure 10 shows the structure's response to the earthquake using the amplitude method scaling was categorized in *Immediate Occupancy* (IO) level. This is because none of the five earthquakes exceeds the maximum IO limit. Besides, structure's response due to spectral matching method is shown in Figure 11. 3 of the 5 earthquakes showed that the x-axis story drift response of the structure exceeded the maximum IO limit. So, structure was categorized in *Life Safety* (LS) level based to FEMA-356 and the structure was categorized in the *Damage Control* level based to ATC-40.

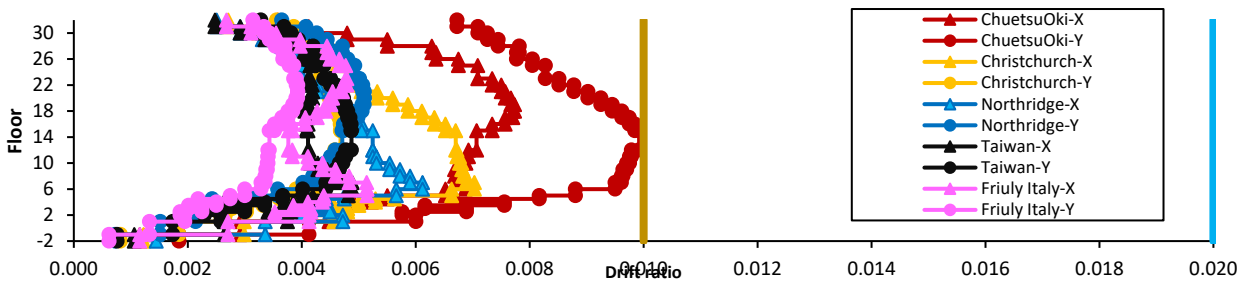

Figure 10. *Interstory inelastic drift ratio of NLTHA with amplitude scaling method*

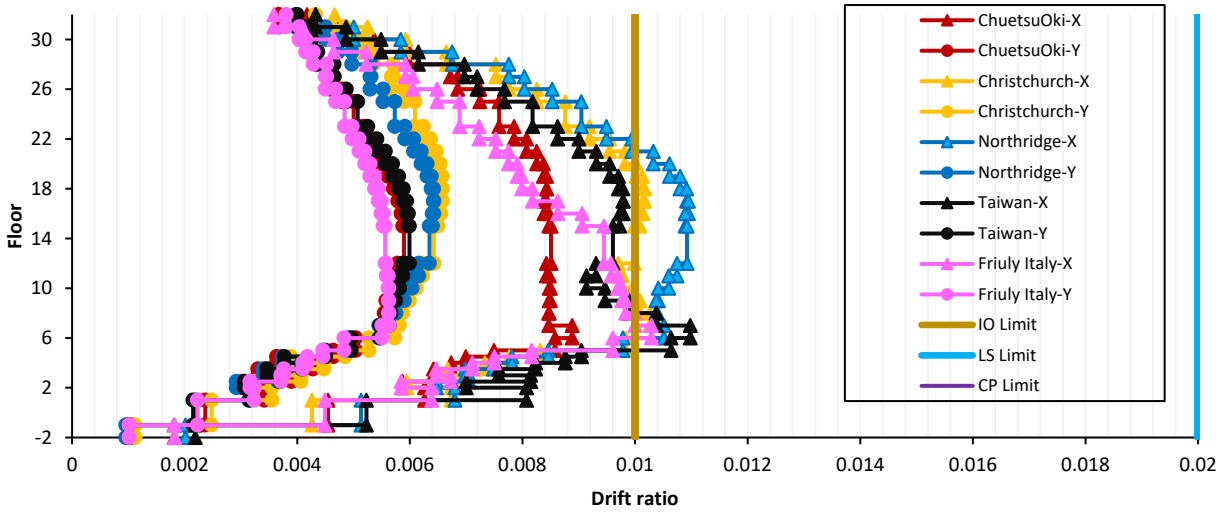

Figure 11. *Interstory inelastic drift ratio of NLTHA with spectral matching method*

B. Structural Element Plasticification

Due to the unreduced earthquake load, the amount of the load capacity exceeds the yield limit of the material's capacity. The plastification occurs because of bending moment that exceeds the yield capacity so that beam do deformation represented by plastic rotation in the z-axis direction until it reaches its ultimate bending moment capacity[23].

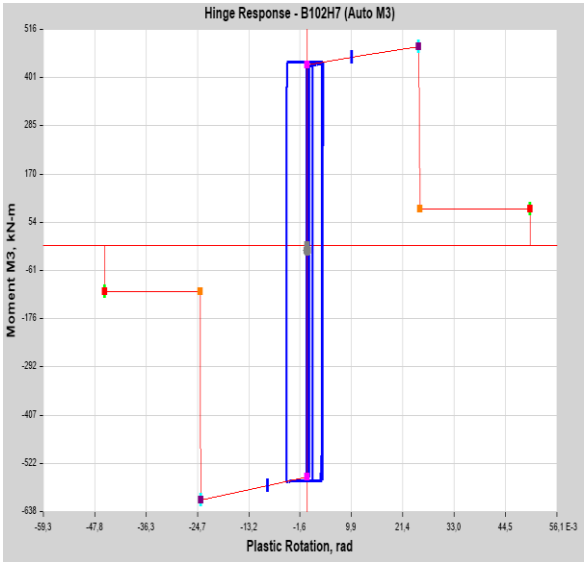

Figure 12. *Beam B2.3 plastic hinge yielding due to Taiwan*

The recapitulation of the plastification all beams is described in table 76. The value of the yield moment calculated by ETABS is compared to the probability yield moment calculated by considering the expected yield stress of $1.25f_y$.

Description in table 7-9:

- AS = Amplitude scaling.
- SM = Spectral matching earthquake
- IO = Limit of immediate rotational occupancy
- LS = Life safety rotation limit
- CP = Rotation limit collapse prevention

Table 7. *Plastification of beam hinges for positive moments*

Plastic Hinge Yielding Because of Positive Moment								
NO	Beam			Capacity		Moment		Ratio
	Type	Floor	As	Mpr+	My(etabs)	AS	SM	
			Joint	kNm	kNm	kNm	kNm	Max (1,1)
1	B1.1	4,5	4-BC	435,9	435,9	444,37	444,37	1,02
2	B1.2	6	1-AB	573,2	573,3	575,4	580,3	1,01
3	B1.3	7	2-CE	592,3	592,4	599,15	605,07	1,02
4	B1.4	6	5-BC	592,3	592,4	617,73	623,75	1,05
5	B1.5	4,5	A-34	592,3	592,4	611,39	607,2	1,03
6	B2.1	5	2'-B'C	296	296,1	302,41	303,98	1,03
7	B2.2	6	2'-B'C	432,2	432,1	451,7	453,25	1,05
8	B2.3	7	2'-B'C	432,2	432,1	451,76	455,66	1,05
9	B4	7	3-C'E	347,4	347,5	353,61	360,38	1,04

Based on information at negative and positive moments described in Table 76-79, no beams experienced failure based on their flexure ability. It was shown that there are no moment yielding ratio that exceeds its maximum Limit (1.1), with the largest ratio obtained is 1.05.

Table 8. *Plastification of beam hinges for positive rotation*

Plastification Rotation because of Positive Rotation									
NO	Balok Beton			AS	SM	*IO*	*LS*	*CP*	Ratio
	Type	Floor	As	θ	θ	θ	θ	θ	
			Joint	rad	rad	rad	rad	rad	
1	B1.1	4,5	4-BC	0,0025	0,00454	0,01	0,025	0,05	IO
2	B1.2	6	1-AB	0,0031	0,00477	0,01	0,025	0,05	IO
3	B1.3	7	2-CE	0,0051	0,00497	0,01	0,025	0,05	IO
4	B1.4	6	5-BC	0,0011	0,00348	0,01	0,025	0,05	IO
5	B1.5	4,5	A-34	0,0001	0,0001	0,01	0,025	0,05	IO
6	B2.1	5	2'-B'C	0,0042	0,00638	0,01	0,025	0,05	IO
7	B2.2	6	2'-B'C	0,0054	0,00635	0,01	0,025	0,05	IO
8	B2.3	7	2'-B'C	0,0052	0,00738	0,01	0,025	0,05	IO
9	B4	7	3-C'E	0,0023	0,00465	0,01	0,025	0,05	IO

Based on the drift's value, no rotation exceeds the IO limit with the largest drift obtained at 0.738%. So that all beam elements are categorized as *immediate occupancy* (IO) level, which means that there are minor structure damages to the beams [7].

The plastification of column is due to the bending moment on the two axes that are strong and weak axes (P-M3 and P-M2). Because of it, a rotation can occur at plastic hinge region of the column [23]. The amount of plastification and the location that occurs in the column are described in table 11.

Table 9. *Plastification at the plastic hinge of the column*

NO	Column			Scenario			
	Type	Floor	As	Aksial			
			Joint	P (kN)	M (kNm)	θ (rad)	Level
1	K1.1	Base	4-A	-24558,5	-13061,3	-0,000001	B-C / IO
2	K2.1	Base	4-B	-25253,8	-6798,1	0	A-B / IO
3	K3.1	Base	3-B	-26648,2	-9744,58	0	A-B / IO
4	K4.1	Base	3-E	-20298,8	-610,611	0	A-B / IO
5	K5.1	Base	5-A	-20215,6	-5359,74	0	A-B / IO
6	K6.1	2	1-D	-17417,2	-2361,14	-0,00207	B-C / IO
7	KB	Base	4-A'	-1744,04	-951,435	0	A-B / IO
8	KL1	Base	3''-C'	-6485,55	-313,233	0	A-B / IO
NO	Column			Scenario			
	Type	Floor	As	Momen			
			Joint	P (kN)	M (kNm)	θ (rad)	Level
1	K1.1	Base	4-A	-6423,1	9070,2	0	A-B / IO
2	K2.1	Base	4-B	-24434,5	-7093,6	0	A-B / IO
3	K3.1	Base	3-B	-26648,2	-9744,6	0	A-B / IO
4	K4.1	Base	4-E	2814,4	1772,7	0,000138	B-C / IO
5	K5.1	2	1-C	-13329,6	-5515,4	0	A-B / IO
6	K6.1	2	1-D	3989,1	4553,6	0,002071	B-C / IO
7	KB	1	5-A'	-1029,5	-1248,9	-0,00011	B-C / IO
8	KL1	Base	3''-C'	2477,0	1035,4	0,002692	B-C / IO

C. Response Modification Factor

The graph drawn in figure 13 that shows structure inelastic behaviour provides information the response limits of the structure under its elastic and plastic conditions. From these limits, data can be obtained on how much the base shear force and the roof drift at the structure's yielding condition, elements first yielding, and the plastic peak of structure. The actual response modification factor of the structure can be determined by evaluate the structure behaviour response that express the relationship between base shear force and roof displacement that occurs at the centre of mass of structure. Figure 13 shows several different curves that represented behaviour response of each scaled ground motion.

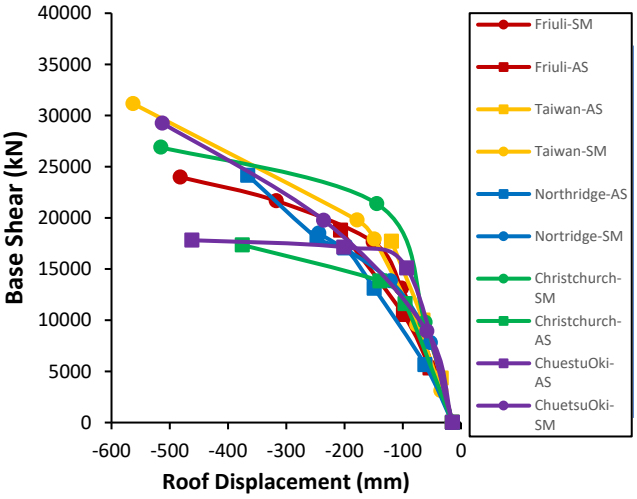

Figure 13. *Base shear–roof displacement response*

The value of the response reduction factor for the influence of structural ductility ($R\mu$) and the response reduction factor for the effect of *over-strength* (*Rs*) is determined by the graph in Figures 13-14. The result of multiplying the two factors will produce actual response modification factor (R).

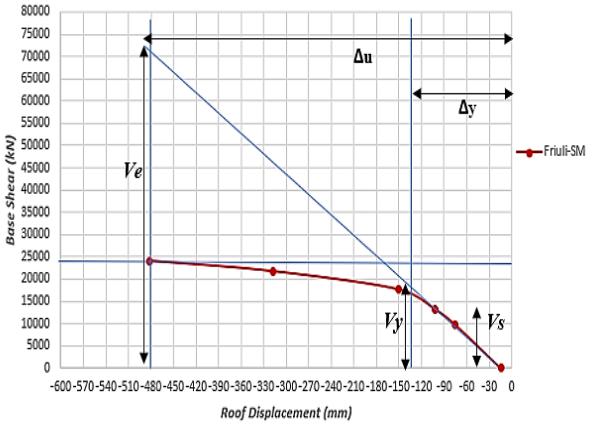

Figure 14. *Procedure for determining R and μ*

The results of the structure's elastic-inelastic response graph are the value of the response modification factor (R) and structure's actual ductility (μ). The two response reduction factors showed synchronous results compared to the evaluation of drift response of the structure. The R(actual) and (actual) values do not exceed the R values used during the design process, which have magnitudes of 7 and 5.5, respectively.

Table 10. *Response modification factor of the x-axis*

Modification	Time history	x-axis responses					
		SNI 1726-2019			actual		
		R	Cd	Ω	$R_{(actual)}$	$Cd_{(actual)}$	$Ω_{(actual)}$
Amplitude Scaling	Northridge	7	5,5	2,5	2,996	2,483	1,086
	Christchurch	7	5,5	2,5	5,028	3,600	1,360
	Chuetsuoki	7	5,5	2,5	5,393	4,742	1,130
	Taiwan	7	5,5	2,5	2,953	1,714	1,283
	Friuli	7	5,5	2,5	3,386	1,873	1,552
Spectral Matching	Northridge	7	5,5	2,5	5,960	3,429	1,424
	Christchurch	7	5,5	2,5	3,160	1,867	1,443
	Chuetsuoki	7	5,5	2,5	5,447	3,667	1,248
	Taiwan	7	5,5	2,5	3,016	1,989	1,278
	Friuli	7	5,5	2,5	4,800	3,708	1,175

Table 11. *Response modification factor of the y-axis*

Modification	Time history	y-axis responses					
		SNI 1726-2019			actual		
		R	Cd	Ω	$R_{(actual)}$	$Cd_{(actual)}$	$Ω_{(actual)}$
Amplitude Scaling	Northridge	7	5,5	2,5	3,942	3,250	1,254
	Christchurch	7	5,5	2,5	3,910	2,520	1,262
	Chuetsuoki	7	5,5	2,5	3,014	3,065	1,195
	Taiwan	7	5,5	2,5	4,733	2,705	1,715
	Friuli	7	5,5	2,5	3,780	2,444	1,654
Spectral Matching	Northridge	7	5,5	2,5	5,692	3,615	1,697
	Christchurch	7	5,5	2,5	6,360	3,478	1,435
	Chuetsuoki	7	5,5	2,5	3,381	2,955	1,146
	Taiwan	7	5,5	2,5	5,236	3,333	1,414
	Friuli	7	5,5	2,5	5,762	2,923	1,822

Conclusion

The results of linear analysis using spectrum response analysis shows that due to changes in the planned earthquake of SNI 1726-2019, predicted inelastic story drift exceed the story drift limit permitted by SNI 1726-2019. Several types of beams experienced overload capacity over their material capacity due to the enlargement of the design earthquake because of updated standard.

Based on story drift ratio, the performance level of the structure is classified in *life safety* (LS) category with largest drift ratio is 1.1% due to the Taiwan-spectral matching earthquake. Meanwhile, based on the plastification of the structural elements, element system are classified in intermediate occupancy (IO) level based on FEMA-356 and ATC-40. According to FEMA-356, the structure under review still meets the maximum allowable limit which is *life safety* (LS), for apartment buildings with risk category II classement against a 500-year plan earthquake.

The reduction factor of elastic structure response expressed in R(actual), Cd(actual), and Ω(actual) sequentially is 6.11, 4.74, and 1.82. While amount of inelastic response reduction factor determined by SNI 1726-2019 which represented as R, Cd, and, Ω sequentially is 7, 5.5, and 2.5.

References

V. A. Harnindra, B. Sunardi, and B. J. Santosa, “Implikasi Sesar Kendeng Terhadap Bahaya Gempa dan Pemodelan Percepatan Tanah di Permukaan di Wilayah Surabaya,” J. Sains dan Seni ITS, vol. 6, no. 2, 2017, doi: 10.12962/j23373520.v6i2.27603.

D. R. Teruna, “Comparison of Seismic Responses for Reinforced Concrete Buildings with Mass and Stiffness Irregularities Using Pushover and Nonlinear Time History Analysis

Comparison of Seismic Responses for Reinforced Concrete Buildings with Mass and Stiffness Irregular," IOP Conf. Ser. Mater. Sci. Eng. Pap., vol. 180, pp. 1–9, 2017, doi: 10.1088/1742-6596/755/1/011001.

K. Suprapto and S. Sudarto, "Evaluation of Performance of Asymmetrically Dual System Structures Using Pushover and Time History Analyses," J. Civ. Eng., vol. 29, no. 1, p. 36, 2009, doi: 10.12962/j20861206.v29i1.1737.

L. H. Najafi and M. Tehranizadeh, "Ground Motion Selection and Scaling in Practice," Period. Polytech. Civ. Eng., vol. 59, pp. 233–248, 2015.

D. I. Wahyudi, "Selecting and Scaling Ground Motion Record for Designed Spectrume Response Approach," J. Apl. Tek. Sipil, vol. 15, no. 2, p. 67, 2017, doi: 10.12962/j2579-891x.v15i2.3103.

W. Partono, M. Irsyam, I. Dwi Atmanto, A. Retno Ari Setiaji, S. Purnomo, and R. Yanuar Setiawan, "Building evaluation using two components of acceleration time histories causes by shallow crustal fault earthquakes with maximum magnitude 7 Mw," in MATEC Web of Conferences, 2018, vol. 195. doi: 10.1051/matecconf/201819502011.

J. P. L. Ngenge and A. M. S. Wafi, "Assessment of plastic hinge in RC structures with and without shear walls applying pushover analysis," Int. J. Adv. Eng. Sci. Appl., vol. 1, no. 1, pp. 11–18, 2020, doi: 10.47346/ijaesa.v1i1.27.

G. I. Marliyani, J. R. Arrowsmith, and K. X. Whipple, "Journal of Geophysical Research : Earth Surface," J. Geophys. Res. Earth Surf. Res., vol. 121, pp. 2287–2308, 2016, doi: 10.1002/2016JF003846.

A. Widodo, F. Syaifuddin, W. Lestari, and D. D. Warnana, "Earthquake potential source identification using magnetotelluric data of Kendeng thrust Surabaya area," E3S Web Conf., vol. 156, 2020.

A. Widodo, F. Syaiffudin, A. Perdana, and T. A. Adausy, "Semi-probabilistic Method in Analysing Kendeng Fault Earthquake Hazard in Surabaya , East Java Semi-probabilistic Method in Analysing Kendeng Fault Earthquake Hazard in Surabaya , East Java," IOP Conf. Ser. Earth Environ. Sci. Pap., vol. 799, 2021, doi: 10.1088/1755-1315/799/1/012026.

R. Sabrin, M. Al, A. Siddique, and K. Sohel, "Seismic Performance Assessment of Existing RC Frames with Different Ultimate Concrete Strains," Civ. Eng. J., vol. 4, no. 6, pp. 1273–1287, 2018.

L. Xian, H. Liu, and Z. Zhao, "Assessing Seismic Collapse Safety and Retrofitting Low-Ductility RC Frame Structures on the Basis of the Acceptable Collapse Safety Margin in China," Appl. Sci., vol. 10, 2020.

V. Soltangharaei, M. Razi, and M. Gerami, "Comparative evaluation of behavior factor of SMRF structures for near and far fault ground motions," Period. Polytech. Civ. Eng., vol. 60, no. 1, pp. 75–82, 2016, doi: 10.3311/PPci.7625.

W. Z. LI Yanjun, LU Dagang, "Ductility reduction factor analysis of RC frames considering influences of infilled walls Ductility reduction factor analysis of RC frames considering influences of infilled walls," in IOP Conference Series: Earth and Environmental Science, 2021. doi: 10.1088/1755-1315/760/1/012060.

I. Journal, E. Sciences, and I. Chief, "PERFORMANCE BASED SEISMIC DESIGN OF STRUCTURES – A REVIEW," Int. J. Eng. Sci. Res. Technol., vol. 9, no. 12, pp. 69–83, 2020.

R. Yadav, T. Gupta, and R. K. Sharma, "Performance Levels of RC Structures by Non-Linear Pushover Analysis," J. Eng. Res. Appl., vol. 7, no. 4, pp. 1–8, 2017, doi: 10.9790/9622-0704020108.

T. Sudo, "A Method for Estimating Ground Motion Based Performance Improvement of Fuel Bedrock Cell Hybrid Powered Test on Railway Vehicle Nonlinear Time-history

Analysis of the," QR RTRI, vol. 63, no. 1, pp. 1–6, 2022.
Y. Liu, "Modal-Based Ground Motion Selection Method for the Nonlinear Response Time History Analysis of Reinforced Concrete Shear Wall Structures," Appl. Sci., vol. 11, no. 8230, pp. 1–21, 2021.
M. Hosseini, B. Hashemi, and Z. Safi, "Seismic Design Evaluation of Reinforced Concrete Buildings for Seismic Design Earthquakes Evaluation of Reinforced Concrete Buildings by Using Nonlinear Time History for Near-Source Earthquakes Analyses by Using Nonlinear Time History Analyses," Procedia Eng., vol. 199, pp. 176–181, 2017, doi: 10.1016/j.proeng.2017.09.225.
E. Kalkan and A. K. Chopra, Practical Guidelines to Select and Scale Earthquake Records for Nonlinear Response History Analysis of Structures. 2010.
M. Azodi, M. Banazadeh, and A. Mahmoudi, "Seismic performance assessment of high-rise steel moment frame building with Reinforced Concrete (RC) core wall based on nonlinear time history analysis," Res. Soc. Dev., vol. 11, pp. 1–16, 2022.
C. Xiaoming, D. Jin, and L. Yungui, "Mass proportional damping in nonlinear time-history analysis," 3rd Int. Conf. Mater. Mech. Manuf. Eng., pp. 567–571, 2015.
M. Alhassan and M. Abdelrahim, "Plastic hinge assessment of RC moment-resisting frames," Int. J. Adv. Eng. Sci. Appl., vol. 1, no. 3, pp. 37–41, 2020.